The image quality of the Southern African Large Telescope (SALT)

Darragh E. O'Donoghue[a], Eli Atad-Ettedgui[b], Luis Balona[a], Bruce C. Bigelow[c], John A. Booth[d], Lucian Botha[a], Janus D. Brink[a], David A. H.Buckley[a], Phil Charles[a], Alrin Christians[a], J. Christopher Clemens[e], Lisa A. Crause[a], Steven M. Crawford[a], Geoffrey P. Evans[a], Hitesh Gajjar[a], Yas Hashimoto[a], Malcolm Hendricks[a], Alexei Kniazev[a], Anthony R. Koeslag[a], Willie P. Koorts[a], Herman J. Kriel[a], Nicola S. Loaring[a], Jonathan Love[a], Fred Marang[a], Douglas Metcalfe[a], Brennan Meyer[a], James O'Connor[a], Charl A. du Plessis[a], Lawrence W. Ramsey[f], Encarni Romero-Colmenero[a], Craig Sass[a], Johann C. Scholtz[a], Ramotholo Sefako[a], Sandisa Siyengo[a], Martin Still[a], Ockert J. Strydom[a], Arkadiusz Swat[g], Johann F. Du Toit[h], Petri Vaisanen[a], Martyn Wells[b], Hannah Worters[a,j]

[a]South African Astronomical Observatory, PO Box 9, Observatory 7935, Cape Town, South Africa,
[b]UK Astronomical Technology Centre, The Royal Observatory Edinburgh, Blackford Hill, Edinburgh EH9 3HJ, United Kingdom,
[c]Dept. of Physics, University of Michigan, 450 Church Street, Ann Arbor, Michigan 48109, USA,
[d]McDonald Observatory, University of Texas at Austin, RLM Building, Austin, TX 78712, USA,
[e]Dept of Physics and Astronomy, University of North Carolina, Chapel Hill, NC 27599, USA,
[f]Dept of Astronomy and Astrophysics, Pennsylvania State University, 525 Davey Laboratory, University Park, PA 16802, USA,
[g]European Southern Observatory, Karl-Schwarzschild-Strasse 2, Garching, D-85748, Germany,
[h]SunSpace, PO Box 3183, Matieland 7602, South Africa,
[j]Centre for Astrophysics, University of Central Lancashire, Preston, PR1 2HE, United Kingdom.

ABSTRACT

Construction of the Southern African Large Telescope (SALT) was largely completed by the end of 2005 and since then it has been in intensive commissioning. This has now almost been completed except for the telescope's image quality which shows optical aberrations, chiefly a focus gradient across the focal plane, along with astigmatism and other less significant aberrations. This paper describes the optical systems engineering investigation that has been conducted since early 2006 to diagnose the problem. A rigorous approach has been followed which has entailed breaking down the system into the major sub-systems and subjecting them to testing on an individual basis. Significant progress has been achieved with many components of the optical system shown to be operating correctly. The fault has been isolated to a major optical sub-system. We present the results obtained so far, and discuss what remains to be done.

Keywords: Southern African Large Telescope, SALT, image quality, spherical aberration corrector, SAC, optical aberrations, astigmatism, focus gradient

1. INTRODUCTION

The Southern African Large Telescope (SALT) (http://www.salt.ac.za) is a 10-m class telescope with a fixed-altitude design similar to that of the Hobby-Eberly Telescope (HET) at McDonald Observatory in West Texas. Constructed during the period 2000-2005, the telescope and its instrumentation have been well documented[1-9] in this conference series and elsewhere. (Many additional papers focusing on specific sub-systems are also available and easily found using an ADS search on 'SALT" or 'Southern African Large Telescope'). During 2005, the first science observations were conducted[10] and since then the telescope has been partially in science operations and partially in commissioning. The lengthy commissioning has arisen due to two major factors: (i) throughput inefficiency in the workhorse first generation Instrument, the Robert Stobie Spectrograph (RSS), a low-medium resolution UV/optical spectrograph (previously known

Advanced Optical and Mechanical Technologies in Telescopes and Instrumentation, edited by Eli Atad-Ettedgui, Dietrich Lemke, Proc. of SPIE Vol. 7018, 701813, (2008) · 0277-786X/08/$18 · doi: 10.1117/12.788841

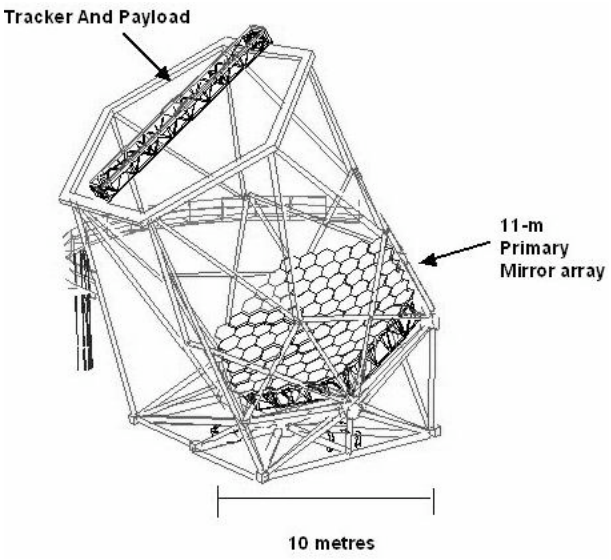

Fig. 1. Basic layout of SALT. The primary mirror comprises 91 hexagonal segments, 1 m in size. The primary is supported on a steel truss mounted in the telescope structure which is tipped over at an angle of 37° to the vertical. At the top of the telescope is a 'Tracker' whose movement capability enables celestial targets to be followed for at least 1 hr, and up to 3 hr at the most southerly declinations.

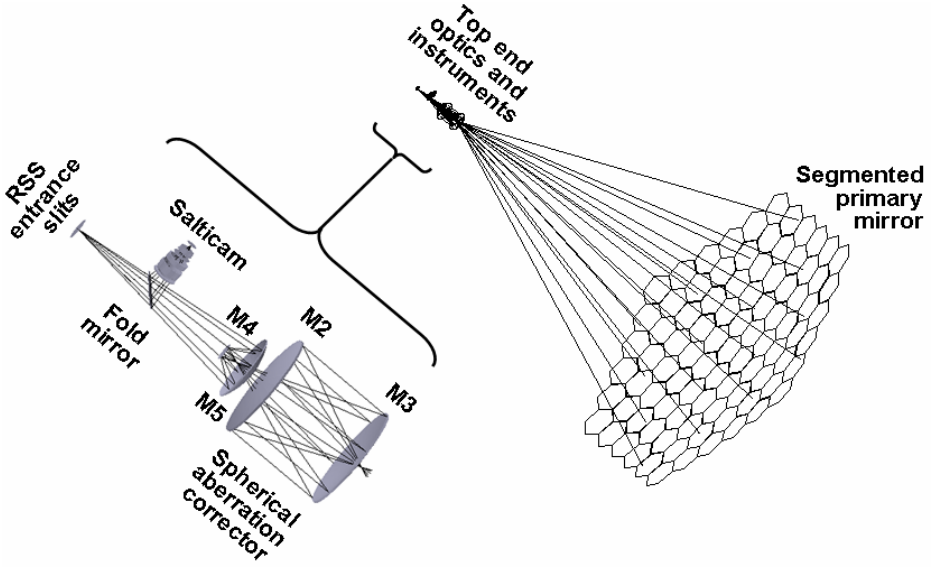

Fig. 2. Optical layout of SALT. At right is shown the primary mirror and top end optics and instruments which are mounted on the Tracker (see Fig. 1). At left is a larger scale view of the top end optics and instruments showing: the 4-mirror spherical aberration corrector (SAC); the Salticam acquisition camera and simple science imager fed by a fold mirror; the "straight-through" focus feeding the slit plane of the Robert Stobie Spectrograph (RSS). In both parts of the diagram, some on-axis rays are traced through the system for the purposes of illustration.

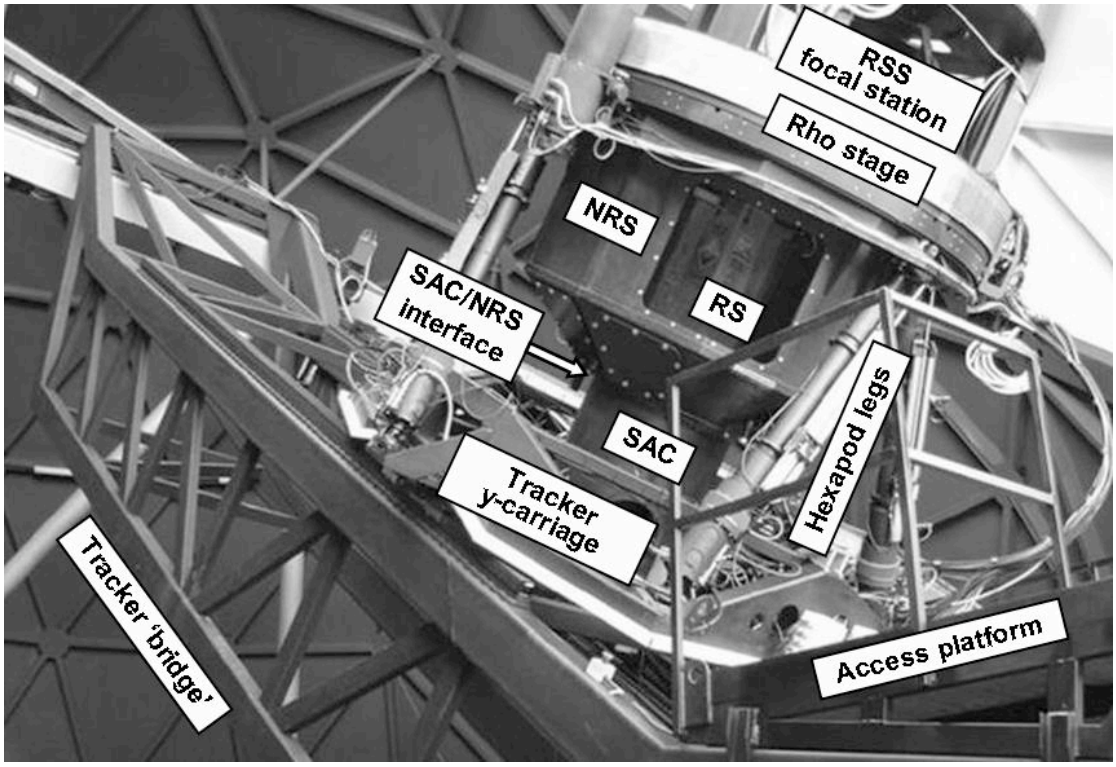

Fig. 3. Physical layout of the SALT top end. Key sub-assemblies are explicitly labeled. See text for description.

as the Prime Focus Imaging Spectrograph (PFIS)); and (ii) problems with the telescope's image quality. This paper describes the nature of the image quality problems, reports an extensive investigation into the causes, shows the progress to date, and discusses what remains to be done. A very detailed account of every step of the investigation appears at http://www.salt.ac.za/iq/the-salt-image-quality-story/.

2. THE DESIGN OF SALT

2.1 The Basic SALT Concept

The basic concept of SALT[1], essentially identical to that of the Hobby-Eberly Telescope, is shown in Fig. 1: a spherical primary mirror, comprising 91 hexagonal spherical segments, is supported by a steel truss mounted in the telescope structure. The telescope structure is able to rotate through 360° in azimuth, but the altitude of the telescope is fixed at 37° from the zenith. If SALT were unable to track, the telescope would therefore only be able to access celestial targets when their zenith distance was exactly 37°. Indeed, during observation, the telescope structure and primary mirror are stationary. However, at the top end of the telescope, incompletely shown as 'Tracker And Payload' in Fig. 1, is a structure which is capable of moving during observations with respect to the axis of symmetry of the primary mirror in six degrees of freedom: x-y decentre, tip, tilt, piston and rotation. This structure, called the 'Tracker', enables the telescope to follow celestial targets over a zenith distance range from 31° to 43°, feeding starlight to the instrument payload. This range of zenith distance corresponds to a track time of at least 1 hr, and up to 3 hr at the most southerly declinations. The same geometrical constraints, along with the -31° latitude of SALT, results in the telescope being able to access targets with declinations only in the range +10° to -72°.

2.2 The SALT Optical Design

As mentioned already, during observation the primary mirror is stationary and the Tracker follows celestial targets over the spherical focal surface of the telescope. This technique requires a spherical primary which in turn drives the optical design of SALT[4]. A 4-mirror spherical aberration corrector[2] (SAC) corrects the huge spherical aberration arising from an

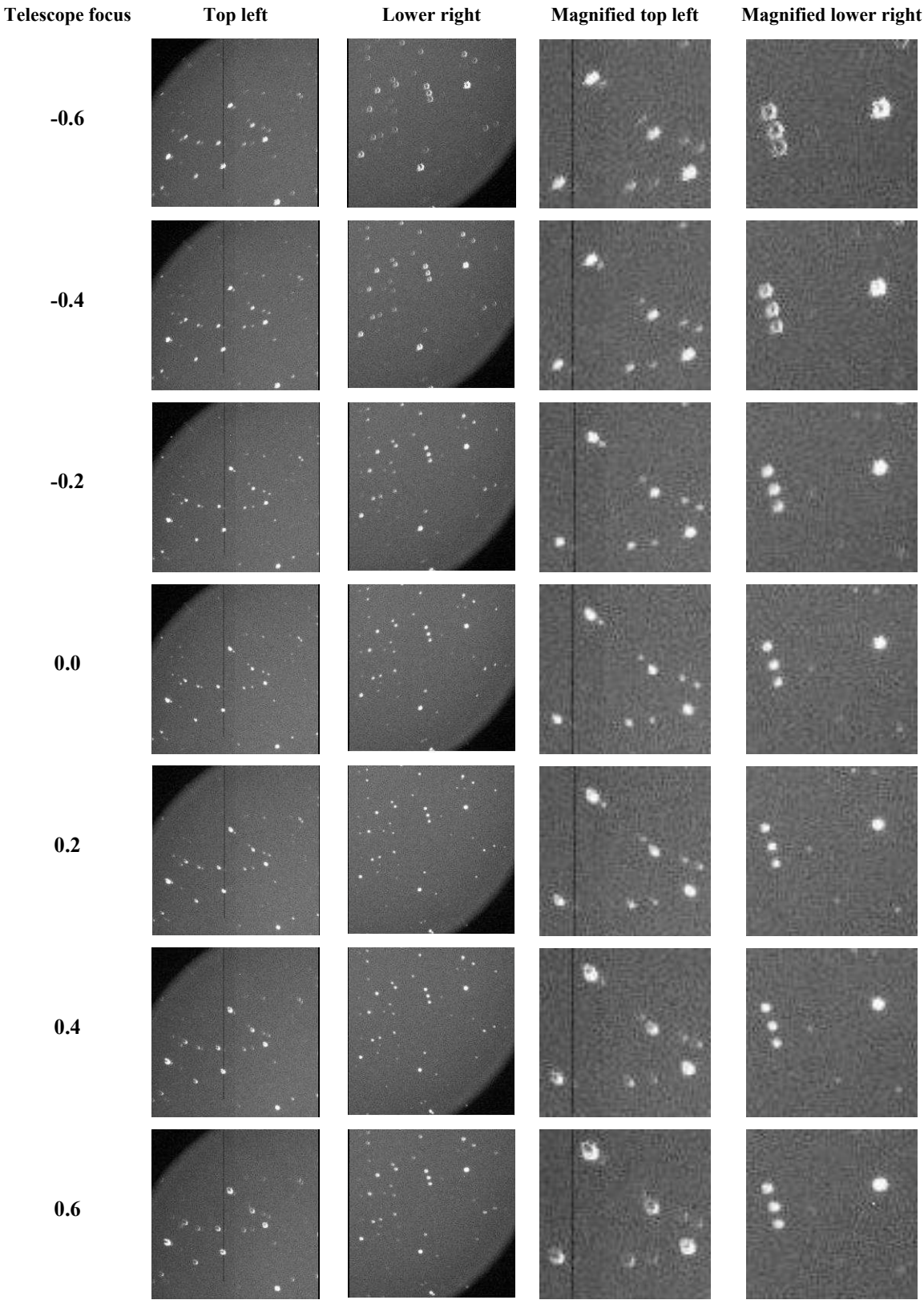

Fig. 4. Sub-images of a "through-focus" sequence illustrating the focus gradient. See text for more explanation.

f/1.4 spherical mirror, 11 m in diameter. The four mirrors, ranging in diameter from 100 mm to 600 mm, are all aspheric with three being conic aspheres, and the fourth, M3, being a general asphere with 1.5 mm of aspheric departure. Fig. 2 shows the SAC layout, with labeling of the SAC mirrors M2-5, and science instruments RSS and Salticam[9,11].

2.3 SALT Top End Layout

In order to appreciate fully the image quality investigation reported in this paper, it is necessary to know the details of the top end of the telescope. These are shown in the photograph in Fig. 3.

As mentioned in Section 2.1, the Tracker follows celestial targets using motions in 6 degrees of freedom: the x translation is achieved by the entire Tracker 'bridge' moving over the top end of the telescope structure; the y motion is achieved by the 'y-carriage' moving up and down the Tracker bridge; tip, tilt and piston are achieved by mounting the payload on 6 hexapod legs whose lengths can be controlled; rotation of the instrument package is achieved using the rho stage (labeled in Fig. 3).

The SAC is mounted at the bottom of a structure made up of carbon fiber panels called the Non-Rotating Structure, labeled NRS in Fig. 3. The NRS is attached at 3 points to a ring at the top of the hexapod legs. As the telescope mount is essentially of the alt-az kind, field rotation during exposure is required, so the rho stage provides this facility for RSS mounted at the top, as well as the contents of the so-called Rotating Structure (RS). The RS is also made up of carbon fiber panels and hangs down from the rho stage inside the NRS. It is labeled RS in Fig. 3 and can be glimpsed through an open hatch door in the NRS. Salticam is located in the RS.

3. THE IMAGE QUALITY PROBLEM

3.1 Symptoms of the problem: focus gradient, astigmatism and variability

Fig. 4 shows some of the symptoms of the image quality problem. Each row of images in Fig. 4 corresponds to a different relative focus position as indicated at the left. The leftmost column in Fig. 4 shows the upper left quarter of a Salticam image (of an arbitrary pointing of the telescope). The column immediately to its right shows the lower right quarter of the same image. The rightmost two columns show sub-images of the leftmost two columns at larger magnification.

The sequence of "through-focus" images shows a differential focus across the field: in the top row both upper left and lower right are out of focus, with the latter more out-of-focus than the former. As the relative focus becomes more positive, the upper left comes to focus first, becoming optimal at a relative focus position of about -0.2. At this position, however, the lower right has still not come to best focus. The lower right is optimal at a relative focus of about +0.2, at which point the focus of the upper left has passed optimal and is worsening. At a relative focus position of +0.6, both upper left and lower right are out of focus, but this time with the upper left more out-of-focus than the lower right. The above behaviour can most easily be understood as a focus gradient over the field. The magnitude of the focus gradient is most easily expressed as the tilt of the RSS entrance slit plane (Fig. 2) required to bring all point source images into simultaneous best focus. This tilt was found to be about 2.5^{o}.

In addition to a focus gradient, there is also astigmatism. A careful inspection of the magnified images in the second column from the right in Fig. 4 (from the upper left corner of the original image) shows that on the more negative side of best focus the stellar images are elongated lower left to upper right, and on the more positive side the images are elongated upper left to lower right. Such behaviour is typical of astigmatism. Astigmatic elongation of stellar images is a very common property of SALT's images.

In addition to focus gradient and astigmatism, the image quality has also been found to be variable: The size of the focus gradient varies, and the astigmatic elongation of point source images also varies. The variation of the focus gradient is about 0.5^{o} about the mean of 2.5^{o}; there is also a variation of the position angle of the focus gradient of about 45^{o}.

Other examples of the complexity of the problem, including images of the globular cluster 47 Tuc, can be found at: http://www.salt.ac.za/iq/the-salt-image-quality-story/image-quality-problem-description/ and http://www.salt.ac.za/iq/the-salt-image-quality-story/exploring-the-focus-dimension-variability/ and http://www.salt.ac.za/iq/the-salt-image-quality-story/odd-looking-stars/

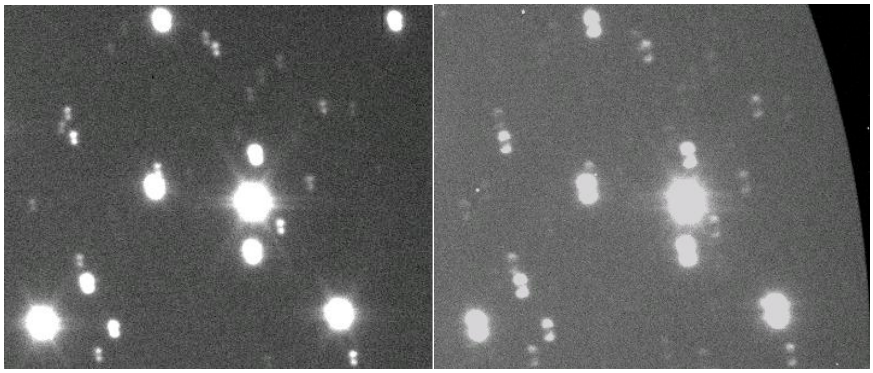

Fig. 5. SALT + science instrument images. On the left is the Salticam image, on the right is the RSS image of the same field, obtained 'quasi-simultaneously' (see text for definition of this term).

4. FIRST STEPS IN DIAGNOSIS

No on-sky image of the full 8-arcmin science field of view had been obtained and no system-level testing of the optical performance of the telescope had been carried out until the last half of 2005. Prior to that time, preliminary on-axis imaging had shown reasonable image quality, so it was a surprise when full-field imaging obtained in 2005 August immediately showed a focus gradient over the field as well as other geometrical aberrations. These problems were initially interpreted as mechanical misalignments of the focal plane and two telescope optical re-alignments were carried out in 2005 Sep and Oct, but without any improvement to the problem. A full-scale investigation was launched at the start of 2006. Tracking down the cause of the problem and fixing it has been SALT's top priority ever since.

4.1 The innocence of the instruments

For the first year of the investigation, the only capability for imaging at the disposal of SALT were the two science instruments RSS and Salticam[9,11] (the latter doubling as the telescope's field acquisition camera). Salticam has re-imaging lenses[11] and RSS has a "straight through" imaging mode using a classic refractive collimator and camera. Although the image quality of both instruments was tested off the telescope prior to installation, their additional lenses might lead to the suspicion that SALT's image quality (IQ) problems arise from them. This, however, was quickly proven not to be the case because:

- It is possible to obtain 'quasi-simultaneous' images with both instruments by flipping in and out the fold mirror shown in Fig. 2 which feeds light to Salticam. When such images were obtained, the *same* aberrations were found in images from both instruments, proving that neither could individually be responsible. A small section of an arbitrary star field is shown in the example images from Salticam (left) and RSS (right) in Fig. 5. Note the doubling of all star images (the apparently single images have saturated lookup tables so their doubling is not apparent). Doubled star images have commonly been seen with SALT, especially on one corner of the science field of view.
- Both instruments rotate with the rho stage. The aberrations are field dependent, so rotation of the rho stage can demonstrate whether or not the origin of the aberrations is in optics which rotate. Images obtained at different values of rho showed the aberrations staying fixed 'on sky' and rotating over the detectors of both instruments. This therefore also proved that the aberrations arise in non-rotating optics.

Further examples and discussion of this topic can be found at http://www.salt.ac.za/iq/the-salt-image-quality-story/first-milestone-the-innocence-of-the-instruments/

From Fig. 2, it is evident that this leaves only the primary mirror and SAC as potential causes of the IQ problems.

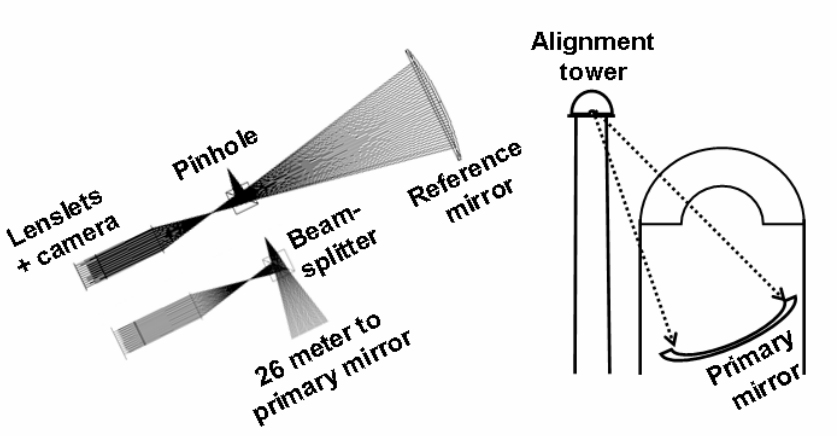

Fig. 6. SALT primary mirror alignment schematic. At the right is a thumbnail sketch of the SALT building and dome containing the primary mirror, as well as the Center-of-Curvature Alignment System (CCAS) tower. Within the CCAS tower is a classical Shack-Hartmann camera which illuminates the spherical primary from a point source (pinhole) located at its centre of curvature. The optical layout is shown in the cartoons at the left: the light proceeds through a beamsplitter to the primary, and returns via the same path to the usual collimator lens and lenslet array. A 'perfect' reference mirror in the other arm of the instrument (top left) provides a reference against which the primary is aligned.

5. COMPREHENSIVE TESTING OF THE PRIMARY MIRROR

The image quality variability, and the doubling of the images evident in Fig. 5, point strongly to the primary mirror as the cause of the IQ problems. This is because, being a segmented spherical mirror, it is aligned (daily) in two halves using a classical Shack-Hartmann camera located at the centre of curvature of the mirror in the so-called Center-of-Curvature Alignment System (CCAS) tower alongside the SALT building, at a distance of 26165 mm from the vertex of the primary's central segment (see Fig. 6). The IQ variability could thus arise naturally from the primary as it is 'reconstructed' daily. In addition, the Shack-Hartmann instrument is not able to 'see' the whole primary simultaneously due to vignetting by the Tracker. The primary is therefore aligned in two halves: by moving the Tracker to the extremes of its x travel, the Shack-Hartmann camera can see each side unvignetted. The central segment is used as the reference to which each side is aligned, and is thus the link between the two halves of the mirror. This modus operandi, if not working correctly for some reason, would naturally give rise to doubling of star images. (Actually a closer inspection of the doubled images shows that they are not 'fully' doubled with *no* light in between the two components; there is some light bridging the components but at a surface brightness several times lower than in either component).

A comprehensive investigation of the performance of the primary mirror was begun. In order to appreciate fully the various aspects of the inquiry, a little more detail about the alignment of the primary is warranted. The CCAS tower is located at azimuth 60^{o} to which the telescope structure is rotated whenever alignment of the primary is required. The Tracker is moved to one extreme of its x range, and the Shack-Hartmann instrument is then used to align the fully visible half of the mirror, after which the other half is aligned with the Tracker at the other end of its x range. The telescope is then available for resuming on-sky observations. Although an edge sensor system to maintain primary alignment was planned for the telescope *ab initio*, a fully operational system has yet to be commissioned so that during the entire IQ investigation reported here, no primary alignment maintenance system was available.

5.1 Testing the primary mirror as the cause of the doubling of star images

The most obvious way for the primary mirror to cause the doubling of star images would involve the incorrect alignment of each side of the mirror. A simple empirical test was devised to check whether or not this was occurring: one side of the primary was not aligned and instead simply "thrown away" by tilting its segments a long way from the aligned, other half. When this was done it was a considerable surprise, therefore, to find that doubling of star images persisted, despite the use of only one side of the primary. It also made no difference which side of the primary was being used. More information on these tests can be found at: http://www.salt.ac.za/iq/the-salt-image-quality-story/testing-the-primary-mirror-i/

5.2 Testing the accuracy of alignment of the primary mirror

Analysis was carried out of the performance of the Shack-Hartmann alignment instrument in the CCAS tower. More specifically, the residuals were analyzed between the spots formed by the return off the primary and the spots formed by the return off the instrument's reference mirror (Fig. 6). These residuals were then inserted into a Zemax model of the telescope incorporating a segmented representation of the primary. Multiple separate sets of residuals from real alignment procedures were used. The outcome was that even the worst cases of alignment were found to give image quality far better than that observed with SALT, and there was no evidence for doubling. Indeed, although the full primary mirror is not visible to the Shack-Hartmann camera at any one time, a substantial part of the vignetted half is visible, and no systematic differences between these segments and the fully visible half were found. More details can be found at: http://www.salt.ac.za/iq/the-salt-image-quality-story/testing-the-primary-mirror-ii/

5.3 Investigating the aberrations of the primary mirror

Zemax simulations were carried out in which the primary mirror, represented as a monolithic, perfectly aligned optical element, had first order coma and/or astigmatism imposed on its figure (assumed to arise from some unspecified cause). The impact of this error in the primary figure on on-sky performance was calculated and found (unsurprisingly as the primary is at the entrance pupil) to be uniform over the science field of view. This conflicts with the symptoms of the IQ problem described in Section 3 in which variations over the field (in both focus and astigmatism) were reported as the most prominent symptoms. More details can be found at: http://www.salt.ac.za/iq/the-salt-image-quality-story/testing-the-primary-mirror-iii/

5.4 "Leg-up" testing of the primary mirror

A potential weakness of the testing of the alignment of the primary mirror as an indicator of its correct working in on-sky observations is that after alignment, the telescope structure has to be moved to some other azimuth to access celestial targets. The primary mirror is supported on a steel truss which in turn is attached to the base wedge of the telescope in a semi-kinematic mount. The base wedge itself has four legs which are set down on an ultra-flat concrete pier. What would the consequences be if the concrete pier were not flat enough? The concrete pier is supposed to be flat to a peak-to-valley variation of no more than 1 mm. In order to investigate the possibility of insufficient flatness of the pier, spacers of 0.6 and 1.2 mm were placed under each of the four legs of the telescope in turn. This procedure was first carried out with the telescope pointing at the CCAS tower (azimuth 60^{o}), so that the Shack-Hartmann alignment instrument could be used to measure the impact of the leg-up spacers on the alignment of the mirror segments. Once again, even in the case of the largest impact (involving a 1.2 mm spacer under leg 2), the misalignment of the primary was found to be insufficient to degrade image quality to that observed with SALT. More details of these tests can be found at: http://www.salt.ac.za/iq/the-salt-image-quality-story/testing-the-primary-mirror-iv/. Further testing of the same kind was also conducted on-sky, which had the advantage that any part of the concrete pier (at any azimuth) could be tested. Again, these tests aroused no concerns that the telescope was unduly sensitive to pier height variations of up to 1 mm.

5.5 On-sky testing in the alignment position

In further pursuit of the possibility of IQ degradation through misalignment of the primary mirror due to moving the telescope structure, on-sky observations while pointing at the CCAS tower were conducted. That this is possible at all is due to the fact that the CCAS tower is slender, and provided the observations are of targets near the centre of the Tracker range, the dome on the tower will fall in the telescope central obscuration. Repeated stacking and on-sky observing were conducted without any movement of the telescope structure. Once again, poor images were seen despite the Shack-Hartmann instrument reporting that the primary mirror was aligned well within its specification of an RMS segment tip/tilt error of no more than 0.07 arcsec. A full report on these tests is available at: http://www.salt.ac.za/iq/the-salt-image-quality-story/testing-the-primary-mirror-v-on-sky-data-at-ccas/.

5.6 Testing the Shack-Hartmann instrument reference mirror

The primary mirror has passed all of the tests described above without raising any suspicions about its correct functioning. The on-sky test is particularly persuasive in making the case that the primary is not responsible for the SALT IQ problems. However, this is only true if the Shack-Hartmann camera in the CCAS tower is working correctly. In particular, the reference mirror (see Fig. 6) must be in good figure otherwise any figure error will then be imposed on the SALT primary. In order to test whether or not there may be problems with the reference mirror, a small test mirror was inserted into the arm of the instrument sending light to the SALT primary (at the position of the label "26 meter to primary mirror" in Fig. 6). Instead of the light traveling 26 m to the SALT primary, it only traveled 200 mm to the test

mirror so that the instrument was then measuring wavefront error between the test mirror and the reference mirror. The result of this test showed that the wavefront error between the two optics had an RMS tip/tilt error of no more than 0.01 arcsec (when scaled up to a tip/tilt error of the SALT segments). The specification for the primary alignment is an RMS tip/tilt error of no more than 0.07 arcsec. So this result proves that the reference mirror is indeed in good optical figure (or the highly unlikely possibility that they both have the same surface figure error). More details can be found at: http://www.salt.ac.za/iq/the-salt-image-quality-story/ccas-testing-the-ccas-instrument-reference-mirror/.

5.7 SPIFFY: the conclusive alibi for the primary

Although a very accurate instrument, the Shack-Hartmann alignment camera discussed above does not give an intuitive feel for the correct operation of the primary. So a simple pinhole/camera combination, called SPIFFY, was installed at the centre of curvature of the primary mirror. Images of the pinhole were formed by the primary on the camera. Typical SPIFFY images were round, not doubled and had a FWHM of about 0.4 arcsec. This is within its specification and much too small to be a contributor to the SALT IQ problem. SPIFFY is also very useful for assessing the state of the primary mirror segment ensemble as the pinhole images from individual segments can be seen separately if each segment is tilted a little away from its neighbours. Variations in radius of curvature and figure for each segment can be measured and monitored, and will no doubt prove to be invaluable as a diagnostic in routine operations. Example images and more information on SPIFFY can be found at: http://www.salt.ac.za/iq/the-salt-image-quality-story/spiffy/.

In the light of its successfully passing all the above tests, there can be little doubt that the primary mirror is not responsible for the SALT IQ problems.

6. THE FOCUS GRADIENT: CAUSES, SIZE AND FIRST ATTEMPT AT A FIX

6.1 Causes of the focus gradient and other symptoms

With the primary mirror eliminated from contention, the SAC was looming large as the primary suspect as the cause of the SALT IQ problems. However, could there be other causes? Before proceeding, it is useful to review all possible causes of the various symptoms of the IQ problem other than the primary mirror.

Table 1. Symptoms and possible causes of the SALT IQ problem.

	Focus gradient	Astigmatism	IQ variability
SAC M2 tip/tilt/decentre	No	No	?
SAC M2 coma	No	No	?
SAC M2 astigmatism	No	Yes	?
SAC M3 tip/tilt/decentre	No	Yes	?
SAC M3 coma	No	No	?
SAC M3 astigmatism	No	Yes	?
SAC M4/M5 tip/tilt/decentre	Yes	Yes	?
SAC M4/M5 coma	Yes	Yes	?
SAC M4/M5 astigmatism	No	Yes	?
Focal plane tip/tilt	Yes	No	?

Table 1 gives such a review. The major IQ problem symptoms are listed at the top of the columns and the leftmost cells in each row show possible causes arising from misalignment or the major first order aberrations coma and astigmatism. Whether or not a cause is capable of giving rise to the symptom is shown as yes or no in the table, and was evaluated using a Zemax model of the telescope, imposing on the various optical elements the indicated misalignment or figure error (coma or astigmatism). The net result of the modeling showed that of the four SAC mirrors, only misalignment or coma in M4 or M5 (see Fig. 1 for the labeling scheme) are capable of generating a focus gradient. Such errors require a compensation for the very large coma generated, but this is easily done by tip/tilting the whole SAC. A focus gradient can also be generated by a focal plane tip/tilt (as is intuitively obvious).

Astigmatism in star images in the focal plane can be generated by misalignment or astigmatism in the figure of mirrors M3, M4 or M5, but not by focal plane tip/tilt. The only rows of the table that have yes in both the second and third

columns have misalignment or coma in the figure of M4 or M5. None of the possible causes naturally give rise to variability in IQ.

6.2 The size of the focus gradient

Measurements of the size and orientation of the focus gradient were made by obtaining sequences of images at different focus positions, determining for each star image the best focus setting, converting that to the appropriate back focal distance, and fitting a plane to the resulting array of back focal distances as a function of position in the focal plane. Sample results are shown in Table 2.

Table 2 Size and orientation of the focus gradient.

Date	No of stars	Focus gradient (deg)	Position angle (deg)
2007 Sep 9	44	2.3 ± 0.1	-61 ± 3
2007 Sep 9	29	2.8 ± 0.3	-59 ± 6
2007 Sep 17	71	2.9 ± 0.1	-45 ± 2
2007 Sep 17	57	2.6 ± 0.2	-84 ± 4
2007 Sep 17	54	2.5 ± 0.1	-53 ± 3

The results show significant variability in the focus gradient from 2.3^o up to 2.9^o with a roughly 45^o variation in position angle where -90^o corresponds to alignment with the Tracker y direction (which is also aligned with gravity).

The magnitude of the focus gradient is, as noted already, very large: the values in Table 2 indicate a mean gradient of about 2.6^o in the detector over the 107 mm science field of view. This corresponds to a variation of back focal distance of 4.9 mm over the field of view. Interpreting the focus gradient as a misalignment of M5, for example, requires a decentre of 0.5 mm or a tip/tilt of 0.1^o in M5 to generate a focus gradient of 2.6^o. Similarly large values are required if M4 is the cause of the focus gradient. These values exceed normal optical tolerances by nearly an order of magnitude!

6.3 First attempt at a fix

As the focus gradient is the most serious source of degradation of image quality over the field, a possible strategy for at least ameliorating the problem is to remove the focus gradient with a simple mechanical tilt of the instruments. This was most easily done by tilting the Rotating Structure (RS: see Fig. 3) by 2.6^o (Table 2). Once this was carried out, however, although the focus gradient was eliminated, the resulting on-sky image quality was worse than before the tilt. The reason for this is not understood.

7. FIRST PROBES OF THE SPHERICAL ABERRATION CORRECTOR (SAC)

7.1 Proving that the SAC is responsible

The elimination of the primary mirror as the cause of the problem leaves the SAC, the last optical sub-system to be independently tested, as the only remaining possibility. With a camera covering the science field of view at the RSS entrance slit position (see Fig. 2), and with SPIFFY providing a simple, quick and intuitive gauge of the performance of the primary mirror, a simple test would prove beyond all doubt that the SAC is responsible for the SALT IQ problems. The camera required was assembled using an Apogee off-the-shelf U9000M peltier-cooled camera with a 4096 x 4096 x 9 μ pixel CCD. The physical size of this CCD is 37 x 37 mm, or 51 mm across the diagonal. This detector was mounted on the x-y table previously used in the Verification Instrument (VI) configuration of Salticam[11]. The x-y table has 3 x 3 discrete positions, and along with the large size of the CCD, the combination covered the 108 mm diameter science field of view of SALT. The procedure used was simple: (i) align the primary mirror; (ii) obtain SPIFFY images showing that the primary is in good figure; (iii) obtain on-sky images with the Apogee in 9 positions of the RSS slit plane; (iv) return to the CCAS tower and use SPIFFY to show that the primary mirror is still in good figure.

The above procedure was executed in 2007 Aug/Sep, verified the good optical state of the primary before and after on-sky imaging which revealed the usual focus gradient and other aberrations. *At last the SAC was proven to be the culprit.* Example images and more information can be found at: http://www.salt.ac.za/iq/the-salt-image-quality-story/proof-that-the-sac-is-responsible/.

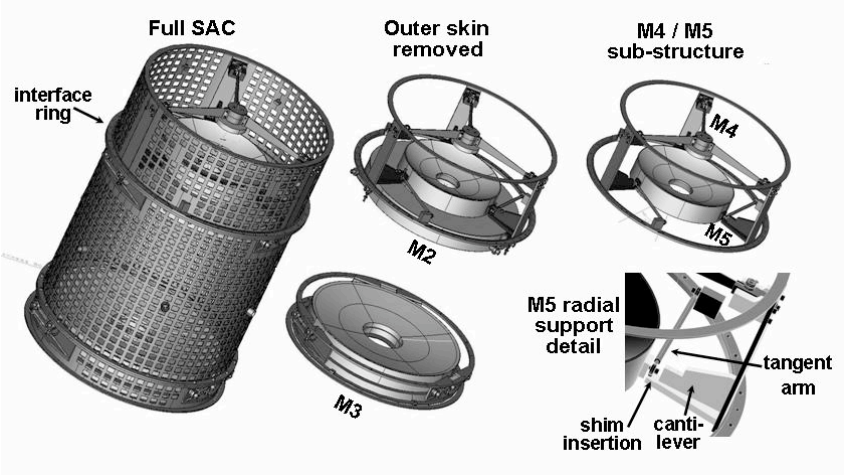

Fig. 7. SAC Breakdown. At left is shown the full SAC which is attached to the NRS by the interface ring (see also Fig. 3). With the outer skin removed, M3 and M2 are revealed with the M4-M5 sub-structure on top of M2 and shown alone at top right. At bottom right is the detail of the M5 radial support: a tangent arm is attached at one end to the upper sub-structure, and at the other end to an invar button bonded to the edge of the glass. Spherical bearings are at either end of the tangent arm. The bearing attached to the invar button sits on an axial support bolt anchored on the cantilever.

7.2 Second attempt at a fix: shimming M5

Within a few months of the beginning of the investigation, it was realized that of the four SAC mirrors, only misalignment of M4 and/or M5 was capable of generating a focus gradient. The comprehensive survey whose results are listed in Table 1 added to the list a coma-type surface distortion of M4 or M5, or tip/tilt of the focal plane. Section 6.3 showed that this was not a viable fix. So with the confidence that the SAC was at fault, and simply as a proof-of-concept, it was decided to tilt M5 in a reversible manner to see if the focus gradient could be eliminated and the other IQ problem symptoms ameliorated. This was executed by inserting a shim of thickness 0.65 mm (!) underneath the spherical bearing on the end of one of the tangent arms supporting M5 – see Fig. 7 and its caption for illustration and explanation of the M5 radial support scheme (as well as a breakdown of the SAC optomechanical system). This did indeed remove the focus gradient and sub-arcsecond star images were produced all over the field. But the gain was short-lived and within a few days, the focus gradient and other aberrations were back. The variability had defeated the attempt at a symptomatic fix and a deeper investigation of the SAC was clearly required. Example images and more information can be found at: http://www.salt.ac.za/iq/the-salt-image-quality-story/shimming-m5/.

8. THE M4-M5 WAVEFRONT TEST

In order to break down the SAC into its subcomponents, an optical test of M4-M5 was devised. A point source placed in the perforation in M5 can be imaged by the M4-M5 pair perfectly stigmatically at the location indicated in Fig. 8: the rays traced in Fig. 8 from the pinhole, reflected off M4 to M5 and thence to the focus, show the optical layout. At the image of the pinhole, either simple array detectors were placed (to form direct images of the pinhole), or a Hartmann wavefront-measuring camera (http://www.okotech.com) to measure the wavefront associated with the image of the pinhole. To place the pinhole roughly, it was mounted in a perspex tube which was inserted through the perforation in M3, with one end located in the perforation in M2, and the other end secured at the perforation in M3.

The exact placement of the pinhole was controlled by an x-y-z array of PI linear stages with 50 nm resolution and 25 mm stroke. To determine where the pinhole should be placed, two lasers and the so-called ‘SAC reference mirror’ (SACRM) were used. First, a downward-shining laser from the CCAS tower was set up to return in autocollimation from the centre of the central segment of the primary mirror. With the downward laser set up in this way, an upward laser from the edge of the primary, reflecting upwards to the CCAS tower off a prism mounted above the primary’s central segment, was adjusted to be collinear with the downward laser. The Tracker and the SACRM were then introduced. The SACRM is a 50 mm diameter flat which can be bolted to an interface on the rear of M4 provided by the SAC supplier. A laser shining from the CCAS tower on to the SACRM, impacting on its centre (as indicated by a scored cross in the optical

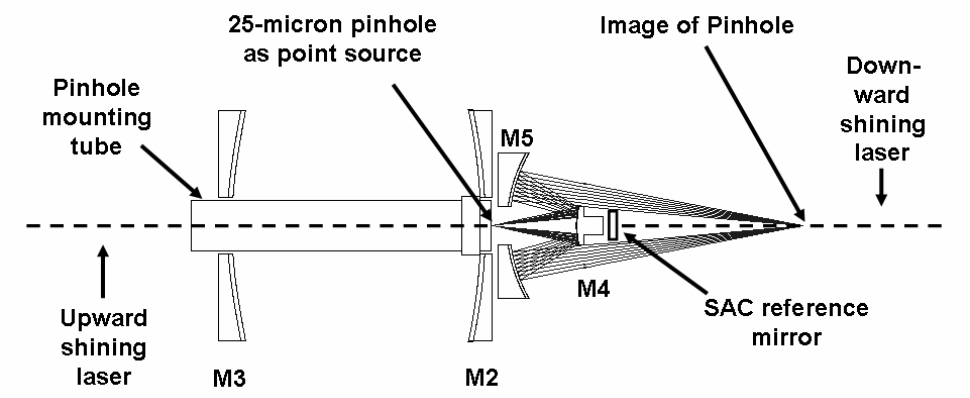

Fig. 8. M4-M5 wavefront test. A 25-micron pinhole mounted at the end of a perspex tube is imaged by M4 and M5. The pinhole is positioned using collinear downward and upward shining lasers (dashed lines) and the SAC reference mirror.

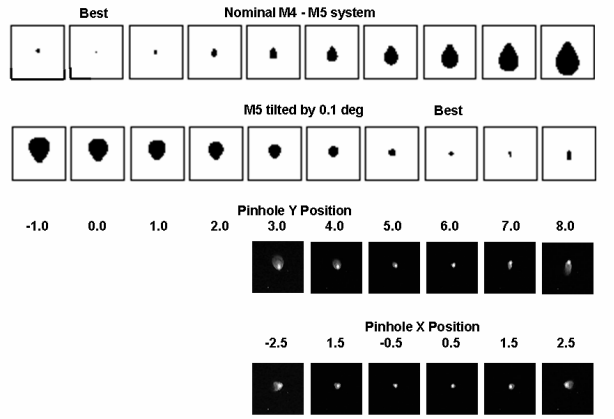

Fig. 9. M4-M5 wavefront test results. The top row shows the images of the pinhole expected for the nominal system for different pinhole y positions (as indicated under the label 'Pinhole Y Position'). The second row shows the images expected if M5 is tilted by 0.1 deg. The third and fourth rows show the real images obtained for x and y pinhole scans.

surface of the mirror) and returning in autocollimation, defines the optical axis of the SAC. The Tracker was thus adjusted in decentre and tip/tilt so that the downward laser returned in autocollimation from the centre of the SACRM. Finally, the pinhole was centred on the upward-shining laser.

The degrees of freedom of the system are limited: the only discretion at the operator's disposal is the x/y positioning of the pinhole. Once placed, the camera (direct or wavefront) has to follow the image of the pinhole (the M4-M5 pair can be thought of as a simple lens imaging the pinhole). If the pinhole is correctly placed, and the surfaces of M4 and M5 are nominal, and M4 and M5 are perfectly aligned, a diffraction-limited image of the pinhole should be realized.

8.1 First results from the M4-M5 wavefront test: misalignment of the mirrors

First results from the test used direct images of the pinhole. What would be expected? The answer to this question, along with the results actually obtained, are shown in Fig. 9. In the top two rows the boxes show Zemax simulations of the expected images of the pinhole for various pinhole positions in the y direction. . The top row shows the nominal system (both M4 and M5 with perfect figures and perfectly aligned). The best image (labeled 'Best') occurs when the pinhole Y position is 0.0 mm (i.e. on axis). This image is diffraction limited. In contrast, if M5 were tilted by 0.1^{o} (a decentre of 0.5 mm has the same effect), the best image occurs when the pinhole is moved off axis by about 6 mm. This image is significantly astigmatic. The third and fourth rows show the observed images from x and y pinhole scans. It is quite clear that the best images in these rows correspond to the misaligned M5 case, and not the nominal system.

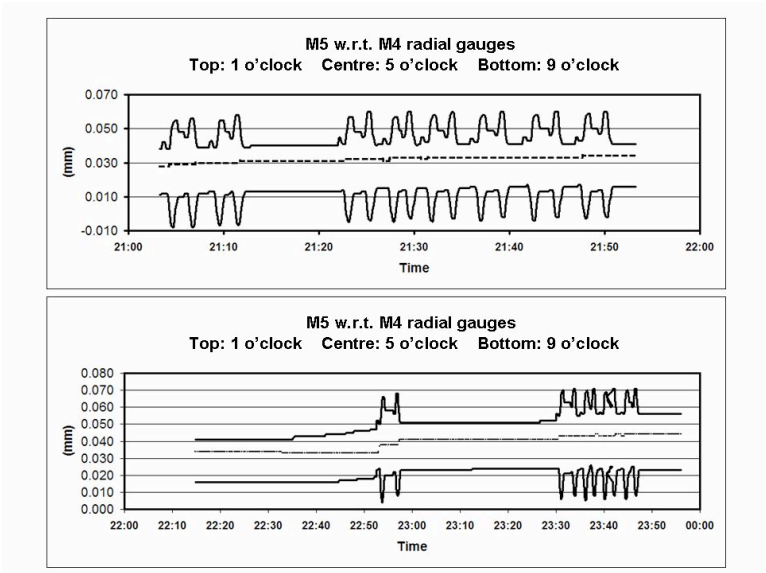

Fig. 10. Dial gauge monitoring over a 3 hr interval of the movement of M5 with respect to M4. See text for details.

Could the placement of the pinhole, on which the result shown in Fig. 9 rests, be uncertain by several mm? The answer is no: wavefront measurements of the pinhole image showed significant astigmatism (Zernike Z5=1.25 waves), confirming that the M4-M5 pair are astigmatic, and consistent with relative misalignment of about 0.1° tip/tilt or 0.5 mm in decentre.

The test setup shown in Fig. 8 was found to be sufficiently stable that wavefront measurements could be made even after exercising all the actuators of the telescope: the telescope structure was thus rotated by 180° and the Tracker moved in all 6 axes, with wavefront measurements being made after each individual movement. It was found that, with the exception of movement of the rho stage (see Fig. 3 and section 2.3), none of these movements had any effect on the images. More information is available at: http://www.salt.ac.za/iq/the-salt-image-quality-story/the-m4-m5-wavefront-test-i/.

8.2 Shimming M5 again

In order to see if diffraction-limited performance for M4-M5 could be restored, shimming M5 was repeated. The shim thickness and orientation were calculated which would remove the astigmatism from the pair. This turned out to be exactly the same as required to remove the on-sky focus gradient (see Section 7.2). Upon re-insertion of the same shim, it was found that the best image required the pinhole to be moved towards the nominal position (see Fig. 9), and that diffraction-limited imaging was indeed achieved. Prior to shimming, the best (astigmatic) wavefront was found to have RMS of 0.36 waves, peak-to-valley of 2.7 waves; after shimming the corresponding numbers were 0.12 and 1.0 waves.

However, once again, this success was short-lived. Within a month the mirror pair was found to form images of the pinhole which were no longer diffraction limited and Z5 had increased to 0.6 waves, about half that seen before.

8.3 Dial gauge monitoring of movements of M4 and M5 and their supports

It was clear by this time that substantial, rapid variability in the optical system was occurring. In order to discover exactly what was causing this, a system of dial gauges was installed in the M4-M5 optomechanical system. For naming purposes, the three support points of M4 and M5 were referred to as "1 o'clock", "5 o'clock" and "9 o'clock" appropriate to their appearance when viewed from the CCAS tower (6 o'clock is the local gravity vector projection).

Three dial gauges were anchored on the three cantilever supports of M5 (see Fig. 7) with their probes touching the edge of M5 (these three will be called group A). In addition, fixturing was installed on the back of M4 with pieces descending to M5 on which were anchored three further gauges (group B), giving measures of the radial movement of M5 with respect to M4. Finally, three further dial gauges (group C) gave the relative movement of M4 with respect to the cantilevers. The gauges provided digital readout every few seconds and were allowed to run for about 5 days. Nothing was moved other than sporadic rotations of the rho stage every few hr. Thermally, the telescope chamber was managed as normal: air conditioning in the day to keep the temperature close to the twilight opening temperature, with the telescope following ambient during the night.

The top panel of Fig. 10 shows the effect of rho rotations on the three group B dial gauges (measuring M5 with respect to M4). Periodic signals (Fig. 10: top) were found, arising from rho stage rotation. Two pulses in Fig. 10 correspond to one cycle of the rho stage from 0^o to 100^o, to -100^o, and back to 0^o. A further remarkable feature is that the gauge at 5 o'clock (central dashed line) does not appear to participate in the motion shown by the other two gauges (upper and lower solid lines). The lower panel of Fig. 10 shows what happens over a longer period of time and with temperature variation induced by controlling the air conditioning. Again, the 5 o'clock gauge does not participate in the motion shown by the other two during the rho rotations, but it does show sudden jumps (just before 23:00), apparently due to the rho movement. These effects raise serious concerns about the optomechanical integrity and stability of the system. In particular, referring back to Fig. 3, and recalling that the SAC is bolted to the bottom of the NRS through its interface ring (see Figs. 3 and 7), the only way that rho rotations can affect M4 and M5 is for stresses to be transmitted down the sides of the NRS from the rho stage, through the interface and into the upper SAC sub-structure and mirror supports.

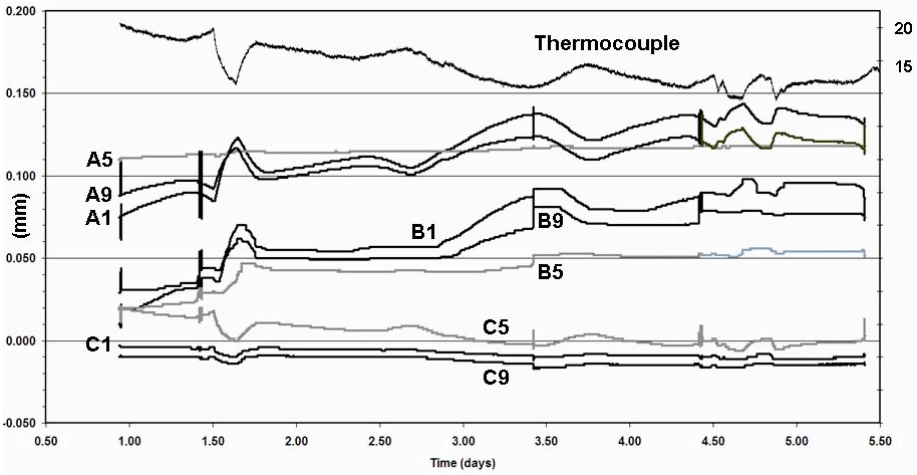

Fig. 11. Monitoring of M5 and M4 by 9 dial gauges over a 5 day interval as described in Section 8.3.

Monitoring of the kind shown in Fig. 10 was conducted for five days. The full results are plotted in Fig. 11. Rho rotations were executed during occasional visits to the telescope by one of us during this time, and are obvious as 'spikes' in the plot. The top curve is the output from an uncalibrated thermocouple in the payload next to the SAC. Over the 5 days the temperature declined by about 10 deg C (as indicated by the rough scale at right). The gauges from each of the groups defined above are indicated by the label closest to the corresponding curve. The most obvious result is a correlation between temperature and the movements of the gauges in groups A and B. In these same two groups, the 5 o'clock gauges (lighter shaded solid line) show the same anomalous behaviour noted previously. There are differential wanderings of considerable size (up to 50 microns) between the gauges of a given group.

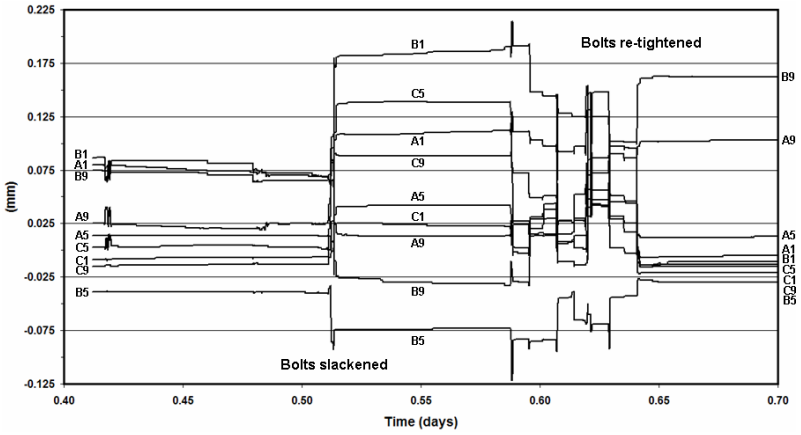

Fig. 12. Monitoring of M5 and M4 by 9 dial gauges during slackening of most of the SAC-NRS mounting bolts. See text.

At the end of the monitoring period shown in Fig. 11, an experiment to de-stress the SAC-NRS interface (see Fig. 3) was conducted. This interface is poorly designed: the SAC interface ring is steel. The ring to which it bolts on the NRS side is made of aluminium, which in turn is bonded into the carbon fibre of the NRS. These are all materials with substantially different CTEs and thermal stresses are inevitable. 21 bolts secure the SAC to the NRS and in the experiment, all but 6 were slackened. The 6 tight bolts were located in 3 groups of 2, spaced apart by 120^{o}. The behaviour of the dial gauges during this procedure is plotted in Fig. 12. Immediately evident are very rapid jumps in the gauges as soon as the bolts were slackened with a large increase in spread. Furthermore, some gauges (A1, B1, A9, B9) did not return to their starting values at the end when the bolts were re-tightened. These symptoms indicate a thermally stressed interface.

9. SUMMARY AND CONCLUSIONS

SALT is contending with serious IQ problems, chiefly a focus gradient as well as astigmatism and other aberrations. Major progress in the diagnosis has been made. We have so far proven that neither the instruments nor the primary mirror are responsible. On the other hand, the spherical aberration corrector is responsible. A large radial misalignment of SAC mirrors M4 and/or M5 (0.1^{o} in tip/tilt or 0.5 mm in decentre) is required. Substantial variability in IQ has also been found, a small part of which arises from mechanical stresses from the NRS being transmitted through the SAC-NRS interface, and the more significant component from thermally-induced stresses in the interface. The fundamental cause is the use of thermally incompatible materials in the SAC mounting interface. A design for a replacement interface, using a kinematic mount or flexures, has already begun, and should be installed in the last quarter of 2008. It is likely that re-alignment of the optics will be needed at that stage. Defining how to do this efficiently is the next major challenge.

REFERENCES

[1] Stobie, R., Meiring, J. and Buckley, D.A.H., "Design of the Southern African Large Telescope (SALT)", Proc. SPIE **4003**, 355-362 (2000)

[2] O'Donoghue, D., "Correction of spherical aberration in the Southern African Large Telescope (SALT)", Proc. SPIE **4003**, 363-372 (2000)

[3] Meiring, J.G., Buckley, D.A.H., Lomberg, M. and Stobie, R., "Southern African Large Telescope (SALT) project, progress and status after 2 years", Proc. SPIE **4837**, 11-25 (2003)

[4] Swat, A., O'Donoghue, D., Swiegers, J., Nel, L. and Buckley, D.A.H., "The optical design of the Southern African Large Telescope", Proc. SPIE **4837**, 564-575 (2003)

[5] Meiring, J.G. and Buckley, D.A.H., "Southern African Large Telescope (SALT) project, progress and status after 4 years", Proc. SPIE **5489**, 592-602 (2004)

[6] Buckley, D.A.H., Hearnshaw, J.B., Nordsieck, K.H. and O'Donoghue, D., "Science drivers and first generation instrumentation for the Southern African Large Telescope (SALT)", Proc. SPIE **4834**, 264-275 (2003)

[7] Buckley, D.A.H., Cottrell, P.L., Nordsieck, K.H. and O'Donoghue, D., "The first-generation instruments for the Southern African Large Telescope (SALT)", Proc SPIE **5492**, 60-74 (2004)

[8] Buckley, D.A.H., Swart, G.P. and Meiring, J.G., "Completion and commissioning of the Southern African Large Telescope", Proc. SPIE **6267**, 564-575 (2003)

[9] Buckley, D.A.H., Burge, E.B., Cottrell, P.L., Nordsieck, K.H., O'Donoghue, D. and Williams, T.B. "Status of the Southern African Large Telescope (SALT) first-generation instruments", Proc. SPIE **6269**, 62690A (2006)

[10] O'Donoghue, D. et al., "First science with the Southern African Large Telescope: peering at the accreting polar caps of the eclipsing polar SDSS J015543.40+002807.2", Mon. Not. R. astr. Soc, **372**, 151-162 (2006)

[11] O'Donoghue, D., E. Bauermeister, E., Carter, D.B., Evans, G.P., Koorts, W.P., O'Connor, J., Osman, F., van der Merwe, S. and Bigelow, B.C. "SALTICAM: A $0.5M Acquisition Camera: Every Big Telescope Should Have One", Proc. SPIE **4841**, 465-476 (2003)